

# An efficient decomposition technique to solve angle-dependent Hanle scattering problems

H. D. Supriya, M. Sampoorna, K. N. Nagendra, B. Ravindra, L. S. Anusha

*Indian Institute of Astrophysics, Koramangala, Bangalore 560034, India*

---

## Abstract

Hanle scattering is an important diagnostic tool to study weak solar magnetic fields. Partial frequency redistribution (PRD) is necessary to interpret the linear polarization observed in strong resonance lines. Usually angle-averaged PRD functions are used to analyze linear polarization. However it is established that angle-dependent PRD functions are often necessary to interpret polarization profiles formed in the presence of weak magnetic fields. Our aim is to present an efficient decomposition technique, and the numerical method to solve the concerned angle-dependent line transfer problem. Together with the standard Stokes decomposition technique we employ Fourier expansion over the outgoing azimuth angle to express in a more convenient form, the angle-dependent PRD function for the Hanle effect. It allows the use of angle-dependent frequency domains of Bommier to solve the Hanle transfer problem. Such an approach is self-consistent and accurate compared to a recent approach where angle-averaged frequency domains were used to solve the same problem. We show that it is necessary to incorporate angle-dependent frequency domains instead of angle-averaged frequency domains to solve the Hanle transfer problem accurately, especially for the Stokes  $U$  parameter. The importance of using angle-dependent domains has been highlighted by taking the example of Hanle effect in the case of line transfer with vertical magnetic fields in a slab atmosphere. We have also studied the case of polarized line formation when micro-turbulent magnetic fields are present. The difference between angle-averaged and angle-dependent solutions is enhanced by the presence of micro-turbulent fields.

*Keywords:* Line: formation - polarization - scattering - magnetic fields - methods: numerical

---

## 1. Introduction

The polarization of line radiation is caused by resonance scattering on bound atomic levels. A modification of this process by external magnetic fields is called the Hanle effect. The linear polarization of strong resonance lines, are particularly sensitive to the type of the frequency redistribution mechanism used in their evaluation especially in the presence of magnetic fields. The differences of the diffuse radiation field between the linear polarization ( $Q/I$ ) profiles computed using angle-averaged and angle-dependent partial frequency redistribution (PRD) functions are illustrated in Faurobert [1] and Sampoorna et al. [2] in the non-magnetic (Rayleigh) case. Nagendra

---

*Email addresses:* `hdsupriya@iias.res.in` (H. D. Supriya), `sampoorna@iias.res.in` (M. Sampoorna), `knn@iias.res.in` (K. N. Nagendra), `ravindra@iias.res.in` (B. Ravindra), `anusha@iias.res.in` (L. S. Anusha)

et al. [3] showed that Stokes  $U$  profiles computed in planar slabs, for the case of Hanle effect, using the angle-averaged PRD functions differ significantly from those computed using angle-dependent PRD functions.

In the case of angle-dependent PRD functions, the strong coupling that exist between the incoming and scattered radiation makes their evaluation and subsequent use in transfer equation numerically expensive. The use of decomposition technique developed by Frisch [4] for the Hanle effect and Frisch [5] for the Rayleigh case, simplifies this numerically expensive problem. In the non-magnetic case Sampoorna et al. [2] used this decomposition technique and developed numerical methods to solve the polarized transfer problem with angle-dependent PRD functions. They also present a detailed historical account of the works on angle-dependent PRD in spectral line polarization. In Sampoorna [6] Hanle transfer problem with angle-dependent PRD was solved using single scattering approximation. Further in Nagendra & Sampoorna [7] (hereafter, NS11) the full Hanle transfer problem with angle-dependent PRD functions was solved by including multiple scattering terms and using scattering expansion method (SEM). It may be noted that SEM was first formulated by Frisch et al. [8] for solving the polarized line transfer equation with complete frequency redistribution (CRD).

In all the above mentioned papers, a Fourier-expansion of the angle-dependent PRD function over azimuth angle difference ( $\chi - \chi'$ ) is employed, where  $\chi$  and  $\chi'$  are the azimuth angles of the outgoing and incoming rays. This technique was first introduced by Domke & Hubeny [9] and was further developed by Frisch [4] for the Hanle transfer problem. The decomposition technique of Frisch [4] allowed the Hanle transfer problem to be solved in an azimuth independent Fourier basis. In NS11 this decomposition technique was used together with the angle-averaged frequency domains (approximation III of Bommier [10]) to solve the Hanle transfer problem with angle-dependent PRD functions. As one has to use in principle, angle-dependent domains themselves for angle-dependent PRD transfer problems, the approach taken in NS11 is inconsistent. Such an approximate approach was taken, because, it allowed to work in an azimuth independent Fourier basis. Clearly in an axisymmetric Fourier basis one cannot apply angle-dependent frequency domains as they explicitly depend on azimuth difference ( $\chi - \chi'$ ). This inconsistency is at the base of the slight differences in the angle-dependent Hanle solutions presented in NS11 (see Fig.4 in that paper), and those presented in Nagendra et al. [3]. Indeed Anusha & Nagendra [11] pointed out that the use of angle-averaged frequency domains for the angle-dependent Hanle transfer problem (as done in NS11) results in a loss of information.

To overcome this inconsistency we adopt Fourier expansion of angle-dependent Hanle PRD matrix over only the outgoing azimuth angle  $\chi$  as suggested in Anusha & Nagendra [11] (see also Anusha & Nagendra [12]). Such an expansion was proposed to solve polarized transfer problems in multi-dimensional media, where the radiation field is non-axisymmetric even in the absence of a magnetic field. In this paper we apply the decomposition proposed by them to the simpler case of polarized transfer in 1D media, and in the presence of a magnetic field. We show that an expansion only over  $\chi$  allows to incorporate angle-dependent frequency domains for angle-dependent PRD functions ‘self consistently’ to solve the transfer problem in the magnetic case.

In Sect. 2 of the paper we describe the decomposition technique employed for the Hanle effect with angle-dependent PRD. In Sect. 3, we discuss the behavior of azimuthal Fourier components of redistribution matrix elements. In Sect. 4, we give the equations of the SEM to solve the Hanle transfer problem. In Sect. 5, we discuss the results obtained by considering our new method of azimuth expansion. A comparison with the results obtained from the perturbation method described in Nagendra et al. [3] and those obtained by using angle-averaged domains (in NS11) is done. In

the same section we also revisit the well known problem of vertical field Hanle effect which arises only due to the angle-dependent PRD in line scattering. Further, we discuss in detail the role of micro-turbulent magnetic fields on line transfer using angle-averaged (AA) and angle-dependent (AD) versions of the redistribution matrix. Conclusions are presented in Sect. 6.

## 2. The decomposition technique

The polarized transfer equation for the Stokes vector can be written in the component form as

$$\mu \frac{\partial I_i}{\partial \tau} = [\varphi(x) + r] [I_i(\tau, x, \Omega) - S_i(\tau, x, \Omega)], \quad (1)$$

where  $i = 0, 1, 2$  refer to the Stokes parameters  $(I, Q, U)$  respectively. The ray direction is given by  $\Omega = (\theta, \chi)$ , with  $\theta = \cos^{-1}(\mu)$  and  $\chi$  being the polar angles.  $x$  is the frequency in non-dimensional units. The line optical depth is denoted by  $\tau$  and  $\varphi(x)$  is the normalized Voigt function  $H(a, x)$ , where  $a$  represents a constant damping parameter. The ratio of continuum to the line absorption coefficient is denoted by  $r$ . The total source vector is given by

$$S_i(\tau, x, \Omega) = \frac{\varphi(x) S_{l,i}(\tau, x, \Omega) + r S_{c,i}}{\varphi(x) + r}, \quad (2)$$

where  $S_{c,i}$  are the components of the unpolarized continuum source vector. We assume that  $S_{c,0} = B_{\nu_0}$ , where  $B_{\nu_0}$  is the Planck function at the line center, and  $S_{c,1} = S_{c,2} = 0$ . The line source vector can be written as

$$S_{l,i}(\tau, x, \Omega) = G_i(\tau) + \int_{-\infty}^{+\infty} \oint \sum_{j=0}^2 \frac{\hat{R}_{ij}(x, \Omega, x', \Omega', \mathbf{B})}{\varphi(x)} I_j(\tau, x', \Omega') \frac{d\Omega'}{4\pi} dx', \quad (3)$$

where  $\Omega' (\theta', \chi')$  is the direction of the incoming ray defined with respect to the atmospheric normal. The solid angle element  $d\Omega' = \sin \theta' d\theta' d\chi'$  where  $\theta' \in [0, \pi]$  and  $\chi' \in [0, 2\pi]$ . The primary source is assumed to be unpolarized, so that  $G_0(\tau) = \epsilon B_{\nu_0}$  and  $G_1(\tau) = G_2(\tau) = 0$ . Here,  $\hat{R}_{ij}(x, \Omega, x', \Omega', \mathbf{B})$  is the Hanle redistribution matrix with angle-dependent PRD, and  $\mathbf{B}$  represents an oriented vector magnetic field. The thermalization parameter  $\epsilon = \Gamma_I / (\Gamma_R + \Gamma_I)$ , with  $\Gamma_I$  and  $\Gamma_R$  being the inelastic collisional de-excitation rate and the radiative de-excitation rate respectively.

In the decomposition method used in this paper, the Stokes vector  $(I, Q, U)$  is first decomposed into a set of six irreducible components  $I_Q^K$ , using which we can construct an infinite set of integral equations for their Fourier coefficients. Following Frisch [4] we can decompose the Stokes source vector into six irreducible components  $S_Q^K$  as

$$S_i(\tau, x, \Omega) = \sum_{K=0,2} \sum_{Q=-K}^{Q=+K} \mathcal{T}_Q^K(i, \Omega) S_Q^K(\tau, x, \Omega), \quad (4)$$

with a similar decomposition for the Stokes vector  $I_i$  in terms of  $I_Q^K$ . The  $\mathcal{T}_Q^K(i, \Omega)$  are irreducible spherical tensors for polarimetry introduced by Landi Degl'Innocenti [13]. The irreducible line source vector components are then given by

$$S_{l,Q}^K(\tau, x, \Omega) = G_Q^K(\tau) + \int_{-\infty}^{+\infty} dx' \oint \frac{d\Omega'}{4\pi}$$

$$\times \frac{1}{\varphi(x)} \sum_{K'=0,2} \sum_{Q''=-K'}^{Q''=+K'} \mathcal{R}_{QQ''}^{KK'}(m, x, x', \Theta, \mathbf{B}) I_{Q''}^{K'}(\tau, x', \Omega'), \quad (5)$$

where  $\Theta [= \cos^{-1}(\mathbf{\Omega} \cdot \mathbf{\Omega}')]$  is the scattering angle,  $G_Q^K(\tau) = (\epsilon B_{\nu_0}, 0, 0, 0, 0, 0)^T$ , and  $\mathcal{R}_{QQ''}^{KK'}$  are the elements of angle-dependent Hanle redistribution matrix given by

$$\begin{aligned} \mathcal{R}_{QQ''}^{KK'}(m, x, x', \Theta, \mathbf{B}) = & \sum_{Q'=-K}^{Q'=+K} [\mathcal{N}_{QQ'}^K(m, \mathbf{B}) R_{\text{II}}(x, x', \Theta) \\ & + \mathcal{N}_{QQ'}^K(m, \mathbf{B}) R_{\text{III}}(x, x', \Theta)] \Gamma_{KQ', K'Q''}(\Omega'). \end{aligned} \quad (6)$$

In this paper we use approximation II of Bommier [10] according to which the redistribution matrix is written as a product of magnetic kernel  $\mathcal{N}_{QQ'}^K(m, \mathbf{B})$  and the angle-dependent redistribution functions  $R_{\text{II,III}}(x, x', \Theta)$  of Hummer [14]. Here the index  $m$  ( $= 1, 2, 3, 4, 5$ ) stands for different frequency domains which depend on  $(x, x', \Theta)$ . The coefficients  $\Gamma_{KQ', K'Q''}(\Omega')$  are defined by

$$\Gamma_{KQ', K'Q''}(\Omega') = \sum_{i=0}^3 (-1)^{Q'} \mathcal{T}_{-Q'}^K(i, \Omega') \mathcal{T}_{Q''}^{K'}(i, \Omega'). \quad (7)$$

The irreducible components  $I_Q^K$  and  $S_Q^K$  and the coefficients  $\Gamma_{KQ', K'Q''}$  are complex quantities. For practical computations, we prefer working with the real quantities. In order to transfer complex quantities into the real space, we follow the procedure given in Frisch [15]. First we define

$$\begin{aligned} I_Q^{K,x}(\tau, x, \Omega) &= \text{Re} \{ I_Q^K(\tau, x, \Omega) \}, \\ I_Q^{K,y}(\tau, x, \Omega) &= \text{Im} \{ I_Q^K(\tau, x, \Omega) \}. \end{aligned} \quad (8)$$

Using these real components it can be shown that  $\mathcal{S}^r = (S_0^0, S_0^2, S_1^{2,x}, S_1^{2,y}, S_2^{2,x}, S_2^{2,y})^T$  and the corresponding intensity vector  $\mathcal{I}^r$  satisfy the transfer equation given in Eq. (1) with  $S_i$  and  $I_i$  replaced by  $\mathcal{S}^r$  and  $\mathcal{I}^r$  respectively. Now using the  $\hat{\mathbf{T}}$  matrix given in Section 5.3 of Frisch [15] the irreducible line source vector in terms of the real quantities can be written as

$$\begin{aligned} S_{l,Q}^{r,K}(\tau, x, \Omega) &= G_Q^K(\tau) + \int_{-\infty}^{+\infty} dx' \oint \frac{d\Omega'}{4\pi} \\ &\times \frac{1}{\varphi(x)} \sum_{K'=0,2} \sum_{Q''=0}^{Q''=+K'} \mathcal{R}_{QQ''}^{r,KK'}(m, x, x', \Theta, \mathbf{B}) I_{Q''}^{r,K'}(\tau, x', \Omega'). \end{aligned} \quad (9)$$

Here  $\mathcal{R}_{QQ''}^{r,KK'}$  has the same form as Eq. (6) with  $\mathcal{N}_{QQ'}^K$  and  $\Gamma_{KQ', K'Q''}$  replaced by  $\mathcal{N}_{QQ'}^{r,K}$  and  $\Gamma_{KQ', K'Q''}^r$ . The  $Q$  indices take values  $[0, +K]$ . The elements of matrix  $\Gamma_{KQ', K'Q''}^r(\Omega')$  are listed in Appendix D of Anusha & Nagendra [16]. The explicit form of  $\mathcal{N}_{QQ'}^{r,K}(m, \mathbf{B})$  can be found in Appendix A of Anusha et al. [17] where they are denoted by  $\mathbf{M}^{(i)}(\mathbf{B})$  with  $i$  playing the role of  $m$  in our notation. The formal solution of the transfer equation can now be written as

$$\begin{aligned} I_Q^{r,K}(\tau, x, \Omega) &= \int_{\tau}^{+\infty} e^{-(\tau' - \tau)\varphi(x)/\mu} S_Q^{r,K}(\tau, x, \Omega) \frac{\varphi(x)}{\mu} d\tau', \quad \text{for } \mu > 0, \\ I_Q^{r,K}(\tau, x, \Omega) &= - \int_0^{\tau} e^{-(\tau' - \tau)\varphi(x)/\mu} S_Q^{r,K}(\tau, x, \Omega) \frac{\varphi(x)}{\mu} d\tau', \quad \text{for } \mu < 0. \end{aligned} \quad (10)$$

The irreducible components of the line source vector in Eq. (9) continue to be non-axisymmetric, because of the presence of angle-dependent redistribution function. It is computationally advantageous to express  $S_{l,Q}^{r,K}$  in terms of axisymmetric irreducible components. This can be achieved through the introduction of Fourier azimuthal expansion of the angle-dependent PRD functions. In this paper we use approximation II of Bommier [10], the expressions of which for the frequency domains depend on the scattering angle  $\Theta$ , and hence on  $\Omega$  and  $\Omega'$ . Therefore, to be consistent, we apply Fourier decomposition to the redistribution matrix which contains the angle-dependent frequency domain information (see Anusha & Nagendra [11]). This can be done as follows:

$$\mathcal{R}_{QQ''}^{r,KK'}(m, x, x', \Theta, \mathbf{B}) = \sum_{k=-\infty}^{k=+\infty} e^{ik\chi} \tilde{\mathcal{R}}_{QQ''}^{(k)KK'}(m, x, x', \theta, \Omega', \mathbf{B}), \quad (11)$$

where the Fourier coefficients are given by

$$\tilde{\mathcal{R}}_{QQ''}^{(k)KK'}(m, x, x', \theta, \Omega', \mathbf{B}) = \int_0^{2\pi} \frac{d\chi}{2\pi} e^{-ik\chi} \mathcal{R}_{QQ''}^{r,KK'}(m, x, x', \Theta, \mathbf{B}). \quad (12)$$

The angle-dependent PRD functions  $R_{\text{II,III}}(x, x', \Theta)$  are periodic functions of  $\chi$  with a period  $2\pi$  because of which each element of the redistribution matrix  $\tilde{\mathcal{R}}_{QQ''}^{(k)KK'}$  is  $2\pi$ -periodic. We remark that in the previous attempts on Fourier decomposition, the expansion of angle-dependent functions  $R_{\text{II,III}}(x, x', \Theta)$  over  $(\chi - \chi')$  was traditionally used (see Domke & Hubeny [9], Frisch [4], Frisch [5]). We show below that an expansion over  $\chi$  of the angle-dependent redistribution matrix (as done in Anusha & Nagendra [11]), provides a consistent way of including ‘angle-dependent frequency domains’ when performing angle-dependent PRD computations. The matrix elements  $\tilde{\mathcal{R}}_{QQ''}^{(k)KK'}$  are studied in detail in Sect. 3. Similar azimuthal Fourier expansions for the primary source term  $G_Q^K(\tau)$  can be written as

$$G_Q^K(\tau) = \sum_{k=-\infty}^{k=+\infty} e^{ik\chi} \tilde{G}_Q^{(k)K}(\tau), \quad (13)$$

with

$$\tilde{G}_Q^{(k)K}(\tau) = \begin{cases} G_0(\tau) & \text{if } k = 0, \\ 0 & \text{if } k \neq 0. \end{cases} \quad (14)$$

Inserting the Fourier azimuthal expansions of  $\mathcal{R}_{QQ''}^{r,KK'}(m, x, x', \Theta, \mathbf{B})$  and  $G_Q^K$  in Eq. (9), we obtain an expansion for  $S_{l,Q}^{r,K}$  which can be expressed as

$$S_{l,Q}^{r,K}(\tau, x, \Omega) = \sum_{k=-\infty}^{k=+\infty} e^{ik\chi} \tilde{S}_{l,Q}^{(k)K}(\tau, x, \theta), \quad (15)$$

with

$$\begin{aligned} \tilde{S}_{l,Q}^{(k)K}(\tau, x, \theta) &= \tilde{G}_Q^{(k)K}(\tau) + \int_{-\infty}^{+\infty} dx' \oint \frac{d\Omega'}{4\pi} \frac{1}{\varphi(x')} \\ &\times \sum_{K'=0,2} \sum_{Q''=0}^{Q''=+K'} \tilde{\mathcal{R}}_{QQ''}^{(k)KK'}(m, x, x', \theta, \Omega', \mathbf{B}) I_{Q''}^{r,K'}(\tau, x', \Omega'). \end{aligned} \quad (16)$$

Substituting from Eq. (15) for  $S_{l,Q}^{r,K}$  in formal solution we get

$$I_Q^{r,K}(\tau, x, \Omega) = \sum_{k=-\infty}^{k=+\infty} e^{ik\chi} \tilde{I}_Q^{(k)K}(\tau, x, \theta), \quad (17)$$

where

$$\begin{aligned} \tilde{I}_Q^{(k)K}(\tau, x, \theta) &= \int_{\tau}^{+\infty} e^{-(\tau'-\tau)\varphi(x)/\mu} \tilde{S}_Q^{(k)K}(\tau, x, \theta) \frac{\varphi(x)}{\mu} d\tau', \quad \text{for } \mu > 0, \\ \tilde{I}_Q^{(k)K}(\tau, x, \theta) &= - \int_0^{\tau} e^{-(\tau'-\tau)\varphi(x)/\mu} \tilde{S}_Q^{(k)K}(\tau, x, \theta) \frac{\varphi(x)}{\mu} d\tau', \quad \text{for } \mu < 0. \end{aligned} \quad (18)$$

Thus from Eqs. (16) and (17) we get an expression for azimuthal Fourier source vector components as

$$\begin{aligned} \tilde{S}_{l,Q}^{(k)K}(\tau, x, \theta) &= \tilde{G}_Q^{(k)K}(\tau) + \int_{-\infty}^{+\infty} dx' \oint \frac{d\Omega'}{4\pi} \frac{1}{\varphi(x')} \\ &\times \sum_{K'=0,2} \sum_{Q''=0}^{Q''=+K'} \tilde{\mathcal{R}}_{QQ''}^{(k)KK'}(m, x, x', \theta, \Omega', \mathbf{B}) \sum_{k'=-\infty}^{k'=+\infty} e^{ik'x'} \tilde{I}_{Q''}^{(k')K'}(\tau, x', \theta'). \end{aligned} \quad (19)$$

Notice that the Fourier indices  $k$  and  $k'$  are not coupled to  $Q$  and  $Q''$  unlike in the case of decomposition over  $(\chi - \chi')$  (see Frisch [4], NS11).

The advantage of working in real irreducible basis is that we can reduce the computational time by restricting the values of azimuthal Fourier index  $k$  to positive space using conjugate symmetry relations as shown below. This simplification is analytically complicated in complex basis. From Eq. (12) we can see that the components  $\tilde{\mathcal{R}}_{QQ''}^{(k)KK'}$  satisfy the symmetry relation

$$\tilde{\mathcal{R}}_{QQ''}^{(k)KK'} = \left[ \tilde{\mathcal{R}}_{QQ''}^{(-k)KK'} \right]^*. \quad (20)$$

Using the above relation in Eq. (11) we get

$$\mathcal{R}_{QQ''}^{r,KK'}(m, x, x', \Theta, \mathbf{B}) = \text{Re} \left[ \sum_{k=0}^{k=+\infty} (2 - \delta_{k0}) e^{ik\chi} \tilde{\mathcal{R}}_{QQ''}^{(k)KK'}(m, x, x', \theta, \Omega', \mathbf{B}) \right]. \quad (21)$$

Notice that the Fourier series constitutes only the terms with  $k \geq 0$  which is useful in practical computations. With this simplification and following as in Eqs. (15)-(19) we get

$$S_{l,Q}^{r,K}(\tau, x, \Omega) = \text{Re} \left[ \sum_{k=0}^{k=+\infty} (2 - \delta_{k0}) e^{ik\chi} \tilde{S}_{l,Q}^{(k)K}(\tau, x, \theta) \right], \quad (22)$$

and

$$I_{l,Q}^{r,K}(\tau, x, \Omega) = \text{Re} \left[ \sum_{k=0}^{k=+\infty} (2 - \delta_{k0}) e^{ik\chi} \tilde{I}_{l,Q}^{(k)K}(\tau, x, \theta) \right]. \quad (23)$$

The  $\tilde{S}_{l,Q}^{(k)K}(\tau, x, \Omega)$  now takes the form

$$\begin{aligned} \tilde{S}_{l,Q}^{(k)K}(\tau, x, \theta) &= \tilde{G}_Q^{(k)K}(\tau) + \int_{-\infty}^{+\infty} dx' \oint \frac{d\Omega'}{4\pi} \frac{1}{\varphi(x)} \sum_{K'=0,2} \sum_{Q''=0}^{Q''=+K'} \tilde{\mathcal{R}}_{QQ''}^{(k)KK'}(m, x, x', \theta, \Omega', \mathbf{B}) \\ &\times \text{Re} \left[ \sum_{k'=0}^{k'=+\infty} (2 - \delta_{k'0}) e^{ik'x'} \tilde{I}_{Q''}^{(k')K'}(\tau, x', \theta') \right]. \end{aligned} \quad (24)$$

### 3. Azimuthal Fourier components of the redistribution matrix elements

In this section we present the azimuth angle dependence of the Fourier decomposed matrix elements of the redistribution matrix, namely  $\tilde{\mathcal{R}}_{QQ''}^{(k)KK'}(m, x, x', \theta, \Omega', \mathbf{B})$ . From Eq. (21), it is clear that the value of  $k$  extends from 0 to  $+\infty$ . For numerical evaluation it is necessary to truncate this infinite series. Our studies show that the series can be truncated at  $k = 4$ . We compute Fourier components  $\tilde{\mathcal{R}}_{QQ''}^{(k)KK'}$  numerically. This we do by numerical integration of  $\mathcal{R}_{QQ''}^{KK'}$  over the azimuth angle  $\chi$  using a Gauss-Legendre quadrature with 32 grid points between  $[0, 2\pi]$ .

Fig. 1 shows the  $\tilde{\mathcal{R}}_{00}^{(k)20}$  element of the redistribution matrix as a function of  $x'$  and  $\chi'$  for a given set of  $x, \theta, \theta'$  and the magnetic field parameters. The main feature is that the  $k = 0$  component is the dominant term. Even though  $k \neq 0$  terms depend sensitively on  $\chi'$ , their magnitudes are several orders smaller than the  $k = 0$  component. For this reason, we can truncate the Fourier azimuthal expansion of the redistribution matrix elements to the fifth term itself without causing significant errors. In fact for practical computation one can truncate the series at  $k = 2$  itself. This would help in rapid computation of the angle-dependent PRD problems in practical applications. However, in the theoretical studies presented in the paper we use  $k = 4$ . From Fig. 1 it follows that the higher order components show several harmonics as  $\chi'$  varies from 0 to  $2\pi$ . This behavior is confined to  $x' \lesssim 3$  when  $x = 0$ . For larger values of  $x'$ , the components approach the value zero. We have verified that the above conclusions remain valid for arbitrary choice of  $x, \theta, \theta'$  and the magnetic field parameters and for other combinations of  $K, K', Q, Q''$ .

### 4. Scattering expansion method for Hanle effect with angle-dependent PRD

In Sect. 3 we showed that the azimuthal Fourier expansion of the redistribution matrix (see Eq. (21)) can be truncated to the fifth term. Thus, for  $k = 0, 1, 2, 3, 4$ , we obtain a finite set of 54 coupled integral equations. The dimensionality of the problem increases to 54 complex quantities from 54 real quantities when we work in full space (i.e.,  $-4 \leq k \leq +4$ ). Thus working in positive half space is computationally advantageous. In this section we present an iterative method to solve this set of coupled equations. This method is based on Neumann series expansion of the components of the source vector contributing to the polarization. Sampoorna et al. [2] applied this method to solve the transfer problem with angle-dependent PRD in non-magnetic case and named it as SEM. These authors also show the efficiency of SEM over the core-wing-based polarized approximate lambda iteration (ALI) method. NS11 employed SEM to solve Hanle transfer problem with angle-dependent PRD. The results obtained by them showed slight inconsistency as compared to the results obtained from perturbation method (Nagendra et al. [3]). This might be due to the use of angle-averaged frequency domains (approximation III) to solve Hanle transfer problem with

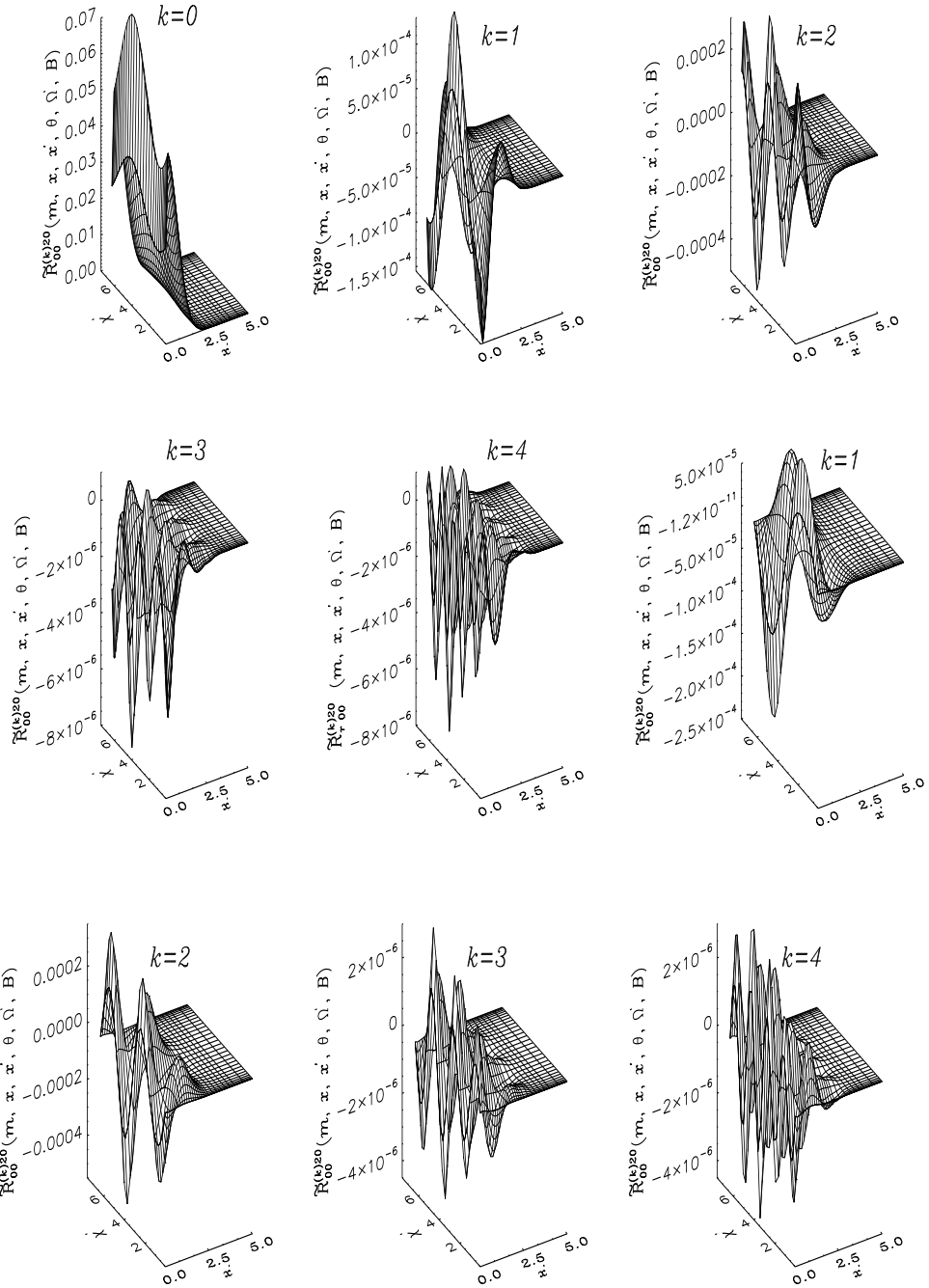


Figure 1: Fourier azimuthal components of the type II redistribution matrix elements are shown as a function of  $x'$  and  $x'$  for  $x = 0$ ,  $\theta = \pi/2$ ,  $\theta' = \pi$  and  $(\Gamma, \theta_B, \chi_B) = (1, 30^\circ, 0^\circ)$ . The first five panels from left to right correspond to the real part of  $\tilde{R}_{00}^{(k)20}$  and the remaining panels refer to the imaginary part of  $\tilde{R}_{00}^{(k)20}$ .

angle-dependent PRD functions. Consistency in the results can be obtained by actually using the angle-dependent frequency domains (approximation II).

In SEM, first neglecting polarization we calculate Stokes  $I$ . We assume that Stokes  $I$  is cylindrically symmetric and is given by the component  $\tilde{I}_0^{(0)0}$  itself to an excellent approximation. This approximation yields  $k' = K' = Q'' = 0$  in Eq. (24). The resulting component is the solution of a non-LTE unpolarized radiative transfer equation with the line source function given by

$$\tilde{S}_{l,0}^{(0)0}(\tau, x, \theta) = \epsilon B_{\nu_0} + \int_{-\infty}^{+\infty} dx' \oint \frac{d\Omega'}{4\pi} \frac{1}{\varphi(x)} \tilde{\mathcal{R}}_{00}^{(0)00}(m, x, x', \theta, \Omega', \mathbf{B}) \tilde{I}_0^{(0)0}(\tau, x', \theta'). \quad (25)$$

Eq. (25) can be solved using a scalar ALI method based on a core-wing approach. Keeping only the contribution of  $\tilde{I}_0^{(0)0}$  on the RHS of Eq. (24) to the  $K = 2$  coefficients and  $k = 0, 1, 2, 3, 4$ , each component  $\tilde{S}_{l,Q}^{(k)2}$  can be written as

$$\left[ \tilde{S}_{l,Q}^{(k)2}(\tau, x, \theta) \right]^{(1)} \simeq \int_{-\infty}^{+\infty} dx' \oint \frac{d\Omega'}{4\pi} \frac{1}{\varphi(x)} \tilde{\mathcal{R}}_{Q0}^{(k)20}(m, x, x', \theta, \Omega', \mathbf{B}) \tilde{I}_0^{(0)0}(\tau, x', \theta'). \quad (26)$$

The superscript 1 stands for the single scattering approximation to the polarized component of the source vector. The corresponding radiation field  $\left[ \tilde{I}_Q^{(k)2} \right]^{(1)}$  for  $k = 0, 1, 2, 3, 4$  is calculated with a formal solver and it serves as a starting solution for calculating the higher-order terms. The higher-order terms can be obtained by substituting for  $\tilde{I}_{Q''}^{(k')2}$  appearing in the RHS of Eq. (24), from  $\left[ \tilde{I}_Q^{(k)2} \right]^{(1)}$ . We see that indices  $k, k', Q$  and  $Q'$  are now decoupled whereas they were coupled in the case of Fourier decomposition over  $(\chi - \chi')$ . Correspondingly the number of non-zero  $\left[ \tilde{I}_Q^{(k)2} \right]^{(1)}$  has increased from 25 to 54 when changing from Fourier expansion over  $(\chi - \chi')$  to that over  $\chi$ . As a result the dimensionality of the problem has increased in the single-scattered solution computation.

In the computation of higher order scattering terms, apart from keeping the coupling of  $(K = 2, Q)$  components with other polarization components ( $K' = 2, Q''$ ), we also keep the coupling of  $k$  with all other  $k'$  terms. We recall that in NS11 coupling of  $k$  with  $k' = 0$  terms were only retained. Thus  $\tilde{S}_{l,Q}^{(k)2}$  at order  $n$  are now given by

$$\begin{aligned} \left[ \tilde{S}_{l,Q}^{(k)2}(\tau, x, \theta) \right]^{(n)} &\simeq \left[ \tilde{S}_{l,Q}^{(k)2}(\tau, x, \theta) \right]^{(1)} + \int_{-\infty}^{+\infty} dx' \oint \frac{d\Omega'}{4\pi} \frac{1}{\varphi(x)} \\ &\times \sum_{Q''=0}^{Q''=2} \tilde{\mathcal{R}}_{QQ''}^{(k)22}(m, x, x', \theta, \Omega', \mathbf{B}) \operatorname{Re} \left\{ \sum_{k'=0}^{k'=+\infty} (2 - \delta_{k'0}) e^{ik' \chi'} \left[ \tilde{I}_{Q''}^{(k')2}(\tau, x', \theta') \right]^{(n-1)} \right\}. \end{aligned} \quad (27)$$

From Fig. 1 it can be seen that  $k = 0$  component of the redistribution matrix elements dominate over the higher order terms ( $k \neq 0$ ). For this reason, despite a strong dependence of  $\tilde{\mathcal{R}}_{QQ''}^{(k)KK'}$  on  $\chi'$ , it is sufficient in the summation over  $k'$  to retain the leading term (namely  $k' = 0$ ) in practical computations. The inclusion of higher order terms  $k' > 0$  do not affect the solutions significantly. Using only  $k' = 0$  term also saves great amount of computing effort.

## 5. Results and discussions

We compare the Stokes parameter  $I$  and the ratios  $Q/I$  and  $U/I$  computed from our present approach with the perturbation method of Nagendra et al. [3] and NS11 approach. The perturba-

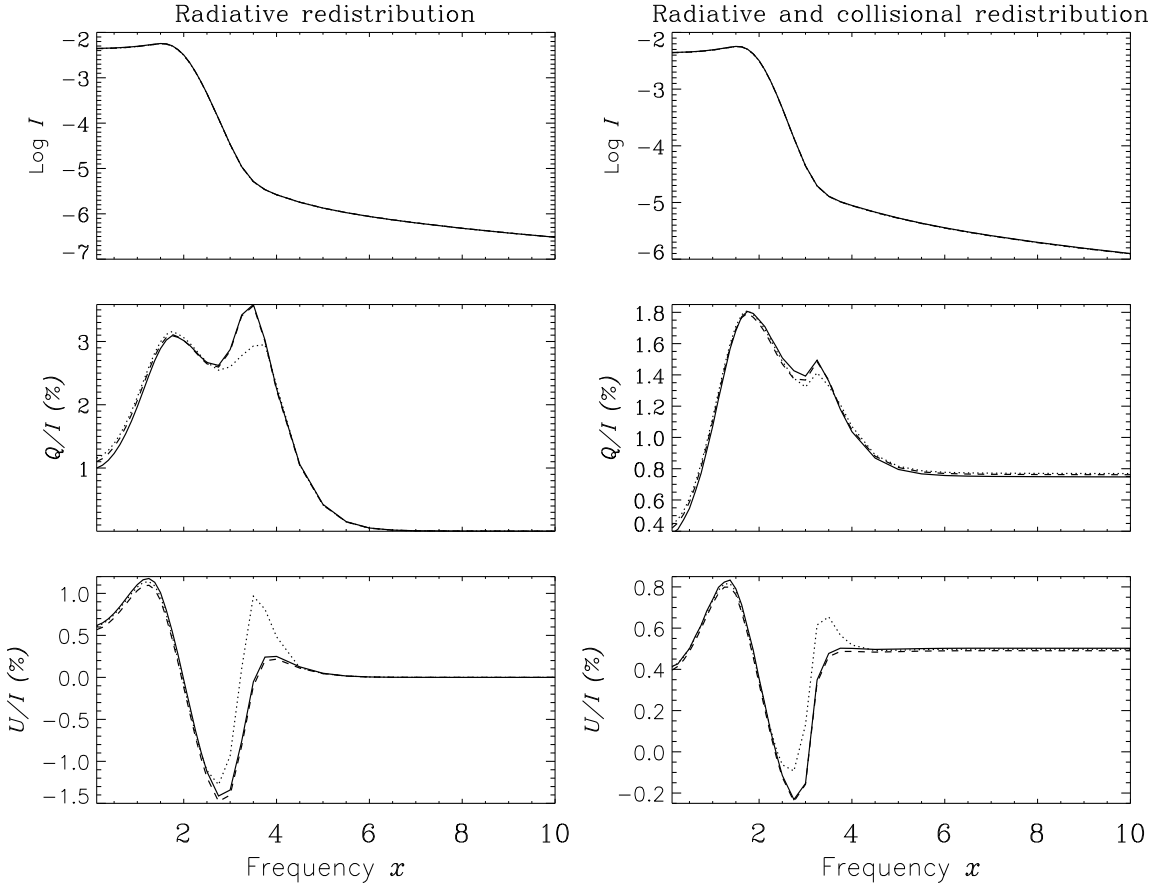


Figure 2: Stokes profiles at  $\mu = 0.112$  computed using three numerical methods, namely the perturbation method (solid line), the NS11 approach (dotted line), and the self consistent approach used in this paper (dashed line). Model parameters are  $(T, a, \epsilon, r, B_{\nu_0}) = (10, 10^{-3}, 10^{-3}, 0, 1)$ . The magnetic field parameters are taken as  $(\Gamma, \theta_B, \chi_B) = (1, 30^\circ, 0^\circ)$ . The left panel shows the results computed using pure  $R_{\text{II}}$  function and the right panel is for a combination of  $R_{\text{II}}$  and  $R_{\text{III}}$  functions with  $\Gamma_E/\Gamma_R = 1$ .

tion method treats linear polarization as a perturbation to the scalar intensity, and computes the polarization in a two step process, wherein an accurately computed Stokes  $I$  is used as an input in evaluation of polarized scattering integral. In successive perturbations, the Stokes  $Q$  and  $U$  are computed more and more accurately until convergence is reached. NS11 approach is discussed in Sections 1 and 5.1. We consider self-emitting plane-parallel, isothermal atmospheres with no incident radiation at the boundaries. The slab models are characterized by  $(T, a, \epsilon, r, B_{\nu_0}, \Gamma_E/\Gamma_R)$ , where  $T$  is the optical thickness of the slab, and  $\Gamma_E$  is the elastic collision rate. The depolarizing collision rate  $D^{(2)}$  is set to  $\Gamma_E/2$ . The plank function  $B_{\nu_0}$  is taken as unity at the line center. The polarizability factor  $W_2$  is taken as unity (i.e, we consider a  $J = 0 \rightarrow 1 \rightarrow 0$  scattering transition with  $J$  the total angular momentum quantum number). The vector magnetic field in the Hanle scattering problem is defined through the field strength parameter  $\Gamma = g\omega_L/\Gamma_R$ , with  $g$  the Landé factor of the upper level and  $\omega_L$  the Larmor frequency; the field inclination  $(\theta_B, \chi_B)$  defined with respect to the atmospheric normal. For angle and frequency discretization we have used quadratures of the same order as those used by NS11. Therefore we do not elaborate here on the computational aspects.

### 5.1. A comparison with previous approaches to solve the angle-dependent Hanle transfer problem

In this section we present the Stokes profiles of the lines formed in a magnetized slab scattering according to Hanle PRD matrix formulated by Bommier [10]. In the so called approximation II and III of Bommier [10], the switch over from the Hanle phase matrices (in the core) to the Rayleigh phase matrix (in the wings) is achieved through the use of angle-dependent and angle-averaged frequency domains respectively. It is shown by Bommier [10] that the use of frequency domains simplifies the numerical evaluation of the redistribution matrices.

It is natural that in AD radiative transfer computations involving AD functions, one should use Approximation II involving AD functions. However, as already discussed in Sects. 1 and 4, in NS11 AA domains were used in computing the AD redistribution matrix. Although such an approach is inconsistent, it provides a rapid means of solving the Hanle AD PRD problems. In the present paper we test their approach by actually using AD frequency domains while computing AD redistribution matrix (which is fully consistent). In Fig. 2, we show a comparison of results obtained by the NS11 and the present approach, along with those obtained from the simple perturbation method of Nagendra et al. [3], which is also consistent, like the present approach. The left panels in Fig. 2 show the Stokes profiles computed using pure  $R_{\text{II}}$  function. One can clearly see that the NS11 approach differs from the present approach particularly in the frequency range  $3 \lesssim x \lesssim 5$ . The present approach and perturbation method give same results. The impact of the approximation used in the NS11 is more severe on the Stokes  $U$  parameter. The right panels in Fig. 2 show the results computed using the same model as in the left panels, but for the introduction of elastic collisions (a combination of  $R_{\text{II}}$  and  $R_{\text{III}}$ ). One can clearly see that the differences between NS11 and the present approach still exist, although the collisions decrease these differences. The present approach, unlike the approximate treatment followed in NS11, thus provides a self-consistent approach to compute the redistribution matrix (i.e., the use of AD domains to compute AD redistribution matrices), at the same time requiring manageable computing resources. This has practical implications in realistic modeling of the observed Stokes profiles.

Table 1 shows a comparison of computing resources required by three numerical methods. Compared to the perturbation method that requires large computing time (112 minutes to obtain a solution), the approximate method of NS11, and the present method are less expensive. In spite of being inconsistent, the approximate method of NS11 requires far less computing memory compared

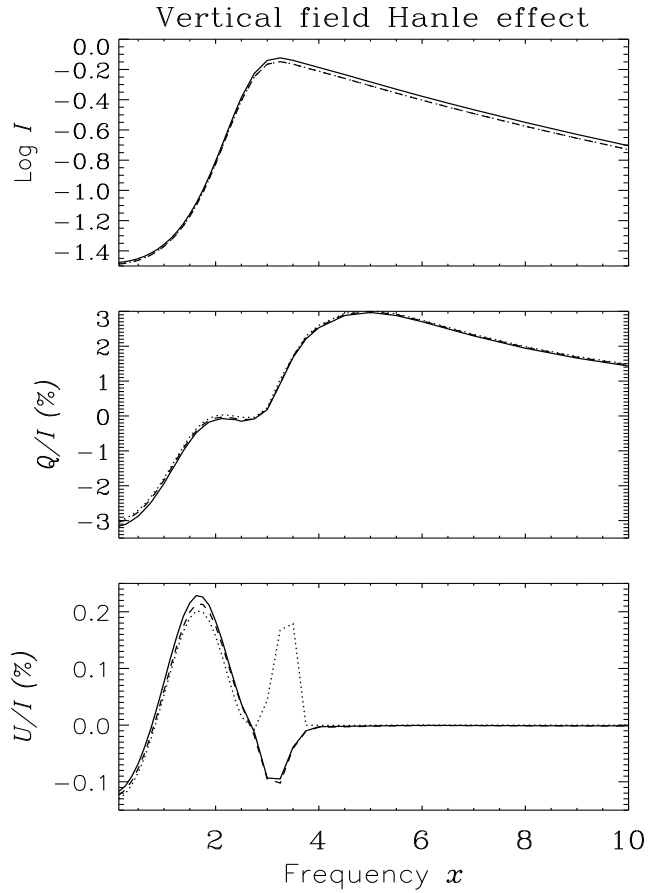


Figure 3: A comparison of emergent Stokes profiles computed by three numerical methods discussed in the text. The profiles are presented for  $\mu = 0.112$  and for a vertical magnetic field  $(\Gamma, \theta_B, \chi_B) = (1, 0^\circ, 0^\circ)$ . Different line types represent same cases as in Fig. 2. The slab model parameters are  $(T, a, \epsilon, r, B_{\nu_0}, \Gamma_E/\Gamma_R) = (2 \times 10^4, 10^{-3}, 10^{-3}, 0, 1, 1)$ .

Table 1: Comparison of CPU time taken by different methods for radiative transfer computations. The model parameters used for the computation are  $(T, a, \epsilon, r, B_{\nu_0}, \Gamma_E/\Gamma_R) = (2 \times 10^6, 10^{-3}, 10^{-3}, 0, 1, 1)$

	Time (minutes)	Memory
Present approach	28	13GB
Perturbation method	112	7.6GB
NS11 approach	33	226MB

to the other two methods. This is because in NS11 the polarized transfer equation is solved in a azimuth independent Fourier basis, which thereby avoids introducing azimuth angle grids. The present approach requires larger memory because we now need to discretize the azimuth angle  $\chi'$  and store the huge matrix  $\tilde{\mathcal{R}}_{QQ''}^{(k)KK'}(m, x, x', \theta, \Omega', \mathbf{B})$ . The memory requirement of the present approach is even larger than that of perturbation method because the former involves solving 54 coupled integral equations in Fourier basis, while the later involves solving 3 coupled integral equations in Stokes basis. However, unlike the present approach the convergence is not always guaranteed in the perturbation method, as angle-frequency coupling is more intricate in Stokes basis than in Fourier basis.

### 5.2. The vertical field Hanle effect

It is expected that when the magnetic field is parallel to the symmetry axis of the slab (the atmospheric normal), the Hanle effect should vanish. In other words the Stokes  $U$  parameter should be zero in this case. This characteristic behavior is satisfied when we work with angle-averaged redistribution functions. When angle-dependent redistribution function is used this behavior is not satisfied. In other words, Stokes  $U$  does not vanish, in spite of the field being vertical, as long as the AD redistribution function is used. The non-zero emergent Stokes  $U$  is due to coupling of Stokes  $U$  to Stokes  $I$  through the components  $\tilde{\mathcal{R}}_{QQ'}^{(k)KK'}$  for  $k \neq 0$ . The reason for this unexpected behavior is also discussed by Frisch et al. [18] and numerically demonstrated in Nagendra et al. [3]. We revisit this interesting problem in Figs. 3 and 4. In Fig. 3 we show the Stokes profiles computed using NS11 and the present approach, and compare it with the results from perturbation method. The differences between the NS11 and the present approach are drastic in Stokes  $U$  parameter. The Stokes  $U$  in the frequency range  $3 \lesssim x \lesssim 5$  has opposite signs. The present approach produces Stokes  $U$  consistent with the perturbation method. The NS11 approach for approximation II seems to be inadequate in computing  $U$  in this particular problem. Such a large difference between the results obtained from NS11 approach and the perturbation method prompts us to conclude that it is safer to use AD frequency domains to solve AD Hanle transfer problems.

Fig. 4 shows the center to limb variation of linear polarization for a vertical magnetic field. The intensity exhibits the characteristic limb darkening in the line core and limb brightening in the wings. The  $Q/I$  shows limb brightening throughout the line profile. The dependence on  $\mu$  is non-monotonic in the core region in  $U/I$ . Since the angle-dependent functions become azimuthally symmetric at the disk center the  $U/I$  approaches zero as the line of sight approaches the disk center. In the line wings,  $U/I$  tend to zero for all  $\mu$ 's which is due to the Rayleigh scattering in the line wings, that produces  $U/I = 0$  by axisymmetry.

### 5.3. The Hanle effect with micro-turbulent magnetic field

It is known that the presence of a weak turbulent magnetic field in the solar atmosphere can be detected using Hanle effect. In the case of CRD, Frisch et al. [8] showed that the polarization

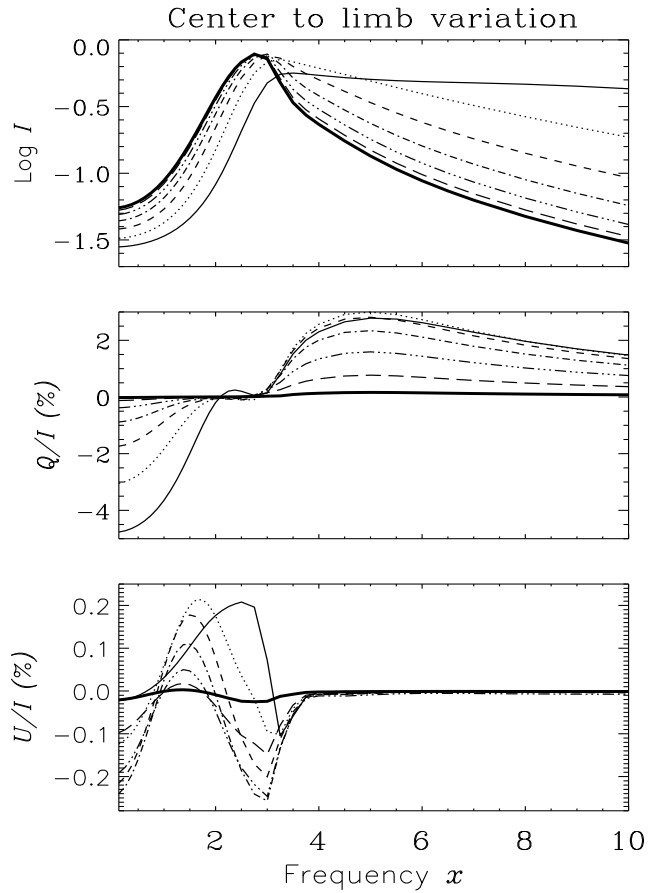


Figure 4: Stokes  $I$  and ratios  $Q/I$  and  $U/I$  for different emergent angles ( $\theta = \cos^{-1} \mu$ ) computed for a vertical magnetic field. The atmospheric model is same as in Fig. 3. Different line types are: solid line -  $\mu = 0.025$ , dotted line -  $\mu = 0.129$ , dashed line -  $\mu = 0.297$ , dot-dashed line -  $\mu = 0.50$ , dash-triple-dotted line -  $\mu = 0.702$ , long-dashed line -  $\mu = 0.871$ , and thick solid line -  $\mu = 0.974$ .

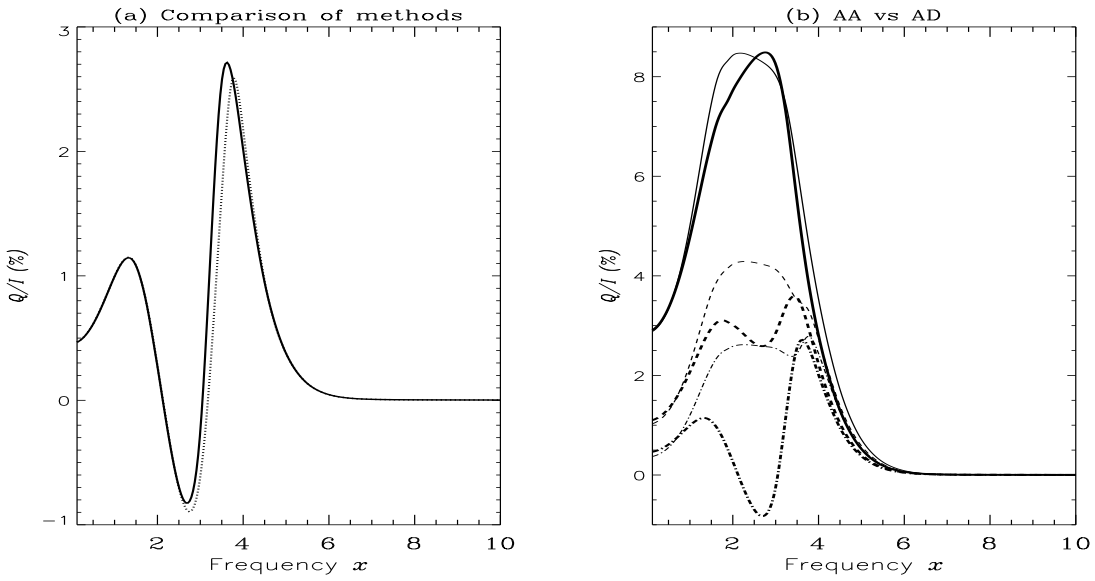


Figure 5: Stokes  $Q/I$  for emergent angle  $\mu = 0.112$  computed for the case of micro-turbulent magnetic field. The atmospheric model is  $(T, a, \epsilon, r, B_{\nu_0}, \Gamma_E/\Gamma_R) = (10, 10^{-3}, 10^{-3}, 0, 1, 0)$ . Panel (a) shows the comparison of the present approach (solid line) and NS11 approach (dotted line). Panel (b) shows the comparison of angle-averaged and angle-dependent cases. Different line types are : non-magnetic case - solid lines; deterministic magnetic field - dashed lines; and micro-turbulent magnetic field - dot-dashed lines. The thick and thin lines represent angle-averaged and angle-dependent cases respectively. For the micro-turbulent magnetic field case,  $\Gamma = 1$  and for the deterministic magnetic field case,  $(\Gamma, \theta_B, \chi_B) = (1, 30^\circ, 0^\circ)$ .

obtained using Hanle effect is quite sensitive to the choice of field strength distribution and in general, micro-turbulence is a safe approximation to represent weak turbulent magnetic fields. For a micro-turbulent magnetic field, the scale of variation of the field is small compared to the mean free path of the photons, and this allows to replace all the field dependent physical parameters by their averages over the magnetic field vector probability density function (PDF). In our problem this condition leads to the averaging of the magnetic kernel  $\mathcal{N}_{QQ'}^{rK}(m, \mathbf{B})$  over the magnetic field vector PDF. In this paper we use a PDF corresponding to the isotropic distribution of field orientation ( $\theta_B$ ,  $\chi_B$ ) and a single value of the field strength. As shown in Stenflo [19, 20] the Hanle problem with this choice of PDF reduces then to a resonance polarization problem, with a modified value of  $Q/I$ . In other words, the micro-turbulent averaged magnetic kernel namely  $\langle \mathcal{N}_{QQ'}^{rK}(m, \mathbf{B}) \rangle$  becomes diagonal, and only  $\langle \mathcal{N}_{00}^{r2}(m, \mathbf{B}) \rangle$  element is of relevance. The explicit form of  $\langle \mathcal{N}_{00}^{r2}(m, \mathbf{B}) \rangle$  is given by (see Appendix B of Frisch et al. [8])

$$\langle \mathcal{N}_{00}^{r2}(m, \mathbf{B}) \rangle = 1 - \frac{2}{5} \frac{\Gamma^2(m)}{1 + \Gamma^2(m)} - \frac{2}{5} \frac{4\Gamma^2(m)}{1 + 4\Gamma^2(m)}, \quad (28)$$

where  $\Gamma(m)$  denotes the Hanle  $\Gamma$ -parameter in different frequency domains. We refer the reader to Eqs. (89) of Bommier [10] for the explicit form of  $\Gamma(m)$  in different frequency domains where Hanle effect is operative. In frequency domains where Rayleigh scattering is present,  $\Gamma(m) = 0$ . Fig. 5 (a) shows the ratio  $Q/I$  obtained using the present approach and the NS11 approach in the presence of micro-turbulent magnetic field. The difference between the results obtained using these different methods mainly exists in the transition region  $3 \lesssim x \lesssim 5$ . Fig. 5 (b) shows the comparison of  $Q/I$  profiles computed using angle-averaged and angle-dependent redistribution matrices. For AA computations, we use redistribution matrices computed in AA domains (approximation III of Bommier [10]), and for AD computations the corresponding AD redistribution matrices are computed in AD domains (approximation II of Bommier [10]). Three different sets of results are presented in Fig. 5 (b), namely non-magnetic, deterministic field, and micro-turbulent field results. We see that in the case of Hanle effect with micro-turbulent magnetic field, there is depolarization in the line core and in the near wing frequencies as compared to the other two cases. Our studies show that in the case of Hanle effect with micro-turbulent magnetic field, the differences between angle-averaged and angle-dependent results are prominent in thin slab cases and reduce considerably in thick slab cases. These differences between AA and AD results, especially in the  $3 \lesssim x \lesssim 5$  region (apart from the line core), were already noticed by Nagendra et al. [3], for the deterministic magnetic field case. It is interesting to note that such differences get enhanced in the presence of a micro-turbulent magnetic field. This is probably because of the localization of line photons within the micro-turbulent scattering eddies, resulting in a relatively larger number of scattering. These differences are present both in the CRD scattering mechanism (see Frisch et al. [8]), as well as PRD as can be seen from Fig. 5 (b).

## 6. Conclusions

We have solved the angle-dependent Hanle scattering problem using angle-dependent partial frequency redistribution (PRD) theory (approximation II of Bommier [10]). This computationally expensive problem is solved using an iterative method based on the Neumann series expansion (SEM). Following Anusha & Nagendra [16] we decompose the Stokes parameters in terms of azimuthally symmetric Fourier coefficients, by expanding the Hanle redistribution matrix in terms of

the radiation azimuth  $\chi$ . Only such a decomposition allows the use of angle-dependent frequency domains for solving angle-dependent Hanle scattering problems. In contrast a decomposition, based on the expansion in terms of  $(\chi - \chi')$ , as done in NS11, does not allow the use of angle-dependent domains to solve angle-dependent Hanle scattering problem. For this reason a simpler approach was suggested by NS11 which used angle-averaged frequency domains (approximation III of Bommier [10]), to solve angle-dependent Hanle transfer problem. We show that their approach does not always hold good. We have carried out a numerical study to show the differences between the solutions obtained by NS11 approach and the self-consistent approach used now in this paper. The  $U/I$  profiles in particular show significant differences in the core to wing transition region ( $3 \lesssim x \lesssim 5$ ) of the line. The special case of vertical field Hanle effect is considered as a case study, and the differences between the NS11 and the present approach are examined. It is shown that the present method offers a self-consistent and accurate method of solving the difficult problem of AD partial redistribution with Hanle scattering. The interesting behavior of  $Q/I$  profiles in the presence of micro-turbulent magnetic fields is also examined. We show that the differences between angle-averaged and angle-dependent solutions are enhanced by the presence of a micro-turbulent field. The differences are noticed in both the line core and near wing regions ( $3 \lesssim x \lesssim 5$ ).

### Acknowledgments

We are grateful to the Referee for very useful and constructive suggestions which helped to greatly improve the paper.

### References

- [1] Faurobert, M. 1988, A&A, 194, 268
- [2] Sampoorna, M., Nagendra, K. N., & Frisch, H. 2011, A&A, 527, A89
- [3] Nagendra, K. N., Frisch, H., & Faurobert, M. 2002, A&A, 395, 305
- [4] Frisch, H. 2009, in Solar Polarization 5, ed. S. V. Berdyugina, K. N. Nagendra, & R. Ramelli (San Francisco: ASP), ASP Conf. Ser., 405, 87
- [5] Frisch, H. 2010, A&A, 522, A41
- [6] Sampoorna, M. 2011, A&A, 532, A52
- [7] Nagendra, K. N., & Sampoorna, M., 2011, A&A, 535, A88 (NS11)
- [8] Frisch, H., Anusha, L. S., Sampoorna, M., & Nagendra, K. N. 2009, A&A, 501, 335
- [9] Domke, H., & Hubeny, I. 1988, ApJ, 334, 527
- [10] Bommier, V. 1997, A&A, 328, 726
- [11] Anusha, L. S., & Nagendra, K. N. 2012, ApJ, 746, 84
- [12] Anusha, L. S., & Nagendra, K. N. 2011b, ApJ, 739, 40
- [13] Landi Degl'Innocenti, E. 1984, Sol. Phys., 91, 1

- [14] Hummer, D. G. 1962, MNRAS, 125, 21
- [15] Frisch, H. 2007, A&A, 476, 665
- [16] Anusha, L. S., & Nagendra, K. N. 2011a, ApJ, 738, 116
- [17] Anusha, L. S., Nagendra, K. N., Bianda, M., Stenflo, J. O., Holzreuter, R., Sampoorna, M., Frisch, H., Ramelli, R., & Smitha, H. N. 2011, ApJ, 737, 95
- [18] Frisch, H., Faurobert, M., & Nagendra, K. N. 2001, in Advanced Solar Polarimetry: Theory, Observation and Instrumentation, ed. M. Sigwarth, ASP Conf. Ser., 236, 197
- [19] Stenflo, J. O. 1982, Sol. Phys., 80, 209
- [20] Stenflo, J. O. 1994, Solar Magnetic Fields (Dordrecht: Kluwer)